Title
Biophysical characterization of microbial rhodopsins with DSE motif.

Journal
Biophysics and Physicobiology, 20(Supplemental)

ISSN
2189-4779

Authors
Marín, María
Jaffe, Alexander
West, Patrick
et al.

Publication Date
2023-03-21

DOI
10.2142/biophysico.bppb-v20.s023

Peer reviewed

Vol. 20, e201023 (2023)
doi: 10.2142/biophysico.bppb-v20.s023

Biophysics and Physicobiology
https://www.jstage.jst.go.jp/browse/biophysico/

Special Issue: Recent Advances in Retinal Protein Research

Regular Article (Invited)

Biophysical characterization of microbial rhodopsins with DSE motif

María del Carmen Marín[1]*, Alexander L. Jaffe[2,3]*, Patrick T. West[2], Masae Konno[1,4], Jillian F. Banfield[5,6,7], Keiichi Inoue[1]

[1]*The Institute for Solid State Physics, The University of Tokyo, Kashiwa, Chiba 277-8581, Japan*
[2]*Department of Plant and Microbial Biology, University of California, Berkeley, CA 94720-3102, USA*
[3]*Department of Earth System Science, Stanford University, Stanford, CA 94305-4216, USA*
[4]*PRESTO, Japan Science and Technology Agency, Kawaguchi, Saitama 332-0012, Japan*
[5]*Innovative Genomics Institute, University of California, Berkeley, CA 94720-2151, USA*
[6]*Department of Earth and Planetary Science, University of California, Berkeley, CA 94720-4767, USA*
[7]*Department of Environmental Science, Policy, and Management, University of California, Berkeley, CA 94720-3114, USA*

Received February 1, 2023; Accepted March 7, 2023;
Released online in J-STAGE as advance publication March 8, 2023
Edited by Yuki Sudo

Microbial rhodopsins are photoreceptive transmembrane proteins that transport ions or regulate other intracellular biological processes. Recent genomic and metagenomic analyses found many microbial rhodopsins with unique sequences distinct from known ones. Functional characterization of these new types of microbial rhodopsins is expected to expand our understanding of their physiological roles. Here, we found microbial rhodopsins having a DSE motif in the third transmembrane helix from members of the Actinobacteria. Although the expressed proteins exhibited blue–green light absorption, either no or extremely small outward H^+ pump activity was observed. The turnover rate of the photocycle reaction of the purified proteins was extremely slow compared to typical H^+ pumps, suggesting these rhodopsins would work as photosensors or H^+ pumps whose activities are enhanced by an unknown regulatory system in the hosts. The discovery of this rhodopsin group with the unique motif and functionality expands our understanding of the biological role of microbial rhodopsins.

Key words: microbial rhodopsins, H^+ pumping activity, flash photolysis, photocycle, metagenomics

Significance

Microbial rhodopsins are photoreceptive membrane proteins with diverse biological functions. The three-residue motif in the third helix plays a critical role in determining their molecular functions. Here, we report DSE motif rhodopsins from members of the Actinobacteria. Regardless of DTD/DTE motifs common in outward H^+ pumping rhodopsins, no or weak outward H^+ pump activity was observed upon light illumination. Most DSE rhodopsin genes make a gene cluster with genes of signaling and metabolic proteins. This suggests that DSE rhodopsins could work either as photosensors or outward H^+ pumps which are regulated by an unknown cellular factor.

*Equally contributed
Corresponding authors: Keiichi Inoue, The Institute for Solid State Physics, The University of Tokyo, Kashiwa, Chiba 277-8581, Japan, https://orcid.org/0000-0002-6898-4347, inoue@issp.u-tokyo.ac.jp; Jillian F. Banfield, Innovative Genomics Institute, University of California, Berkeley, CA 94720-2151, USA, Department of Earth and Planetary Science, University of California, Berkeley, CA 94720-4767, USA, Department of Environmental Science, Policy, and Management, University of California, Berkeley, CA 94720-3114, USA, https://orcid.org/0000-0001-8203-8771, jbanfield@berkeley.edu

Introduction

Microbial rhodopsins are a super-family of heptahelical transmembrane photoreceptive membrane proteins using all-*trans*-retinylidene Schiff base chromophore, so-called all-*trans*-retinal [1–4]. Microbial rhodopsins are present in diverse microorganisms over three domains of life: bacteria, archaea, unicellular algae, fungi, protists, etc., and even in giant viruses [2–4]. Most microbial rhodopsins transport ions using light energy in an active (ion-pumping rhodopsins) or passive (channelrhodopsins) manner [3,5,6]. Additionally, microbial rhodopsins which regulate C-terminally fused enzyme domains or bestrophin ion channel domains are known [7,8].

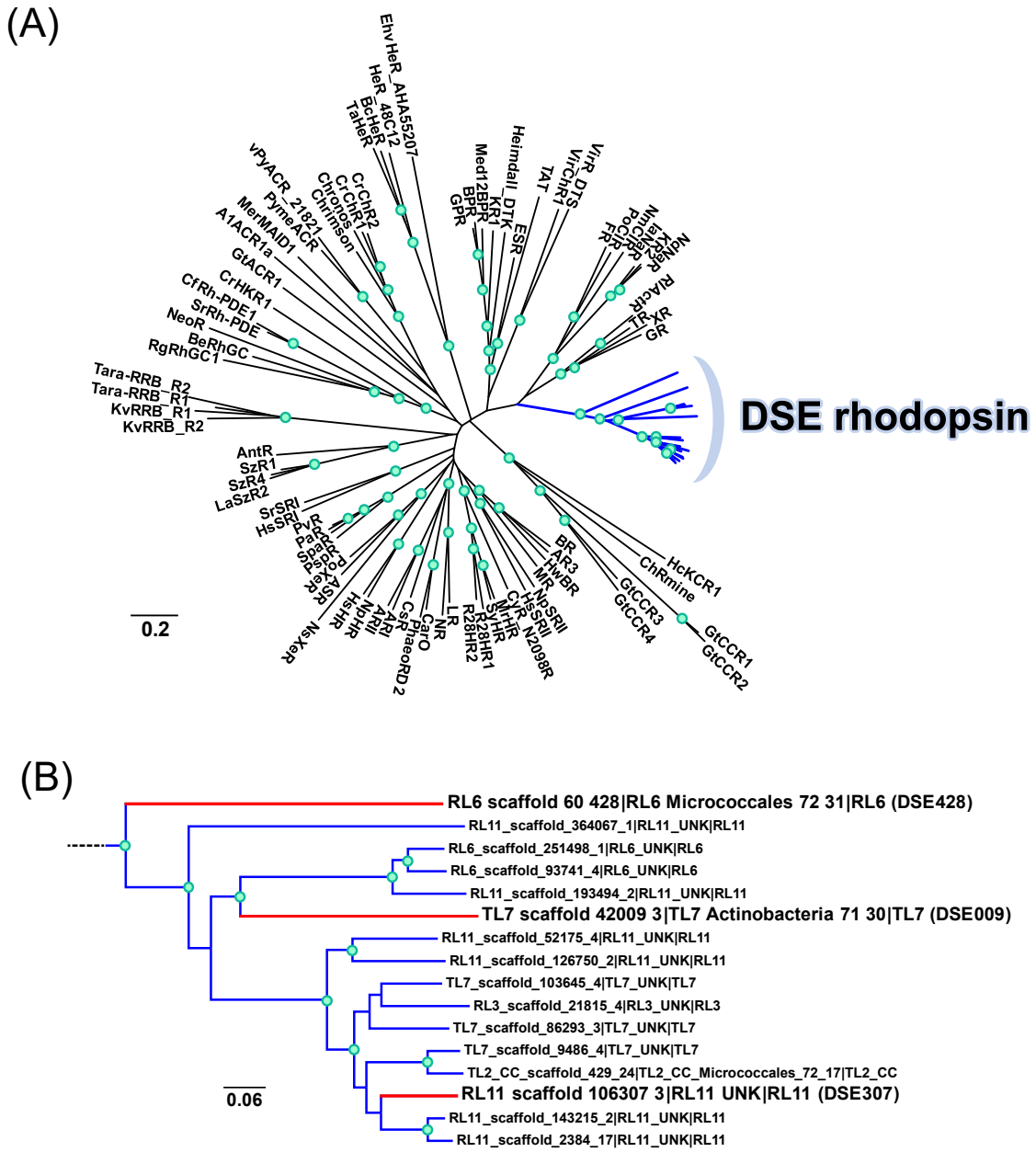

Figure 1 (A) The phylogenetic tree of microbial rhodopsins with DSE rhodopsins. The branch of DSE rhodopsins was shown in blue. (B) Expanded view of the branch of DSE rhodopsins in (A). The branches of the three representative DSE rhodopsins were shown in red. The nodes with bootstrap values ≥80% were indicated by green circles.

Recent progress in genomic and metagenomic analyses on the genomes of microorganisms revealed thousands of novel microbial rhodopsin genes [9–12]. While many rhodopsins having new functionality were found among them, the amino acid residues essential for each function were also identified [2]. One of the most prominent examples of the key amino acid residues is the so-called "motif" residues in the third transmembrane helix (TM3). The canonical outward proton (H^+) pumping rhodopsin, bacteriorhodopsin (BR) from *Halobacterium salinarum* [13], has two highly important aspartic acids, Asp85 and Asp96, on the extracellular and cytoplasmic sides of TM3, respectively [14]. Asp85 is deprotonated in the dark and stabilizes the protonated Schiff base linkage of the retinal chromophore (retinal Schiff base, RSB) as its counterion. The retinal chromophore isomerizes to the 13-*cis* form after light absorption, and then an H^+ is transferred from RSB to Asp85, resulting in the blue shift of the absorption of the chromophore to near-UV region [1]. This blueshifted state is called M state. After the M state, Asp96, which is protonated in the dark, transfers another H^+ to the deprotonated RSB, leading to the outward H^+ transport in concert with the H^+ acceptance of Asp85. With Thr89, which is present between Asp85 and 96 in TM3 and critical in the H^+ transfer between the RSB and Asp85 [15], these residues are called the "DTD motif" [5]. The residues at these positions play critical roles in other types of microbial rhodopsins. Furthermore, there is a substantial correlation between the function and motif types especially in ion-pumping rhodopsins [2,16]: *e.g.*, DTD/DTE/DTK/DTG/DTS: outward H^+ pump [10,17–19], TSA/TSD/TTD/NTQ: inward Cl^- pump [20–23], NDQ: outward H^+ pump [5], FSD/FSE: inward H^+ pump [24], etc. Interestingly, xenorhodopsins (XeR), a group of inward H^+-pumping rhodopsins [25], show diversified motifs (DSX/DTX where X is A, I, L, M S, or T). However, they have a unique proline at a position homologous to BR Asp212 which works as the second counterion of RSB in TM7, suggesting TM7 is important for the functionality of XeR [25].

To explore functionally novel microbial rhodopsins, we comprehensively checked motif residues in the microbial rhodopsins in microbiomes associated with terrestrial lichens and found a new group of 16 rhodopsins having "DSE motif". They are phylogenetically distinct from other microbial rhodopsin groups (Figure 1). All were determined to be derived from members of the Actinobacteria, primarily of the order Micrococcales. Since there is no group of microbial rhodopsins having the same motif, it is difficult to presume the function of DSE rhodopsins. Hence, here we conducted biophysical characterization of three representative DSE rhodopsins, one from Micrococcales: RL6 scaffold 60 428|RL6 Micrococcales 72 31|RL6 (DSE428), one from Actinobacteria: TL7 scaffold 42009 3|TL7 Actinobacteria 71 30|TL7 (DSE009), and one from unknown species: RL11 scaffold 106307 3|RL11 UNK|RL11 (DSE307) (red lines in Figure 1B).

Materials and Methods

Exploration of DSE Rhodopsin Genes

We sampled over 30 lichens from the Angelo Coastal Reserve in northern California, USA to study their eukaryotic and bacterial components. Six individual lichens samples, representing six distinct lichen holobionts from rock and tree substrates, were then selected for metagenomic sequencing. DNA was extracted from each sample and Illumina NovaSeq 2x250PE read sequencing performed, resulting in a total of 713.6 million reads and 178.4 Gbp of total sequencing length (average of 29.7 Gbp of sequencing data per sample). Metagenomic reads were then *de novo* assembled using MEGAHIT v1.2.8 [26]. Protein predictions from assembled scaffolds were made using Prodigal (meta mode) and annotated using USEARCH against the KEGG, UniRef, and UniProt databases. Candidate rhodopsins were extracted by a text-based search of all annotations and subjected to further annotation via kofamscan. Only those candidate rhodopsins that were ≥ 200 amino acids in length and attained best hits to the K04641 (bacteriorhodopsin), K04643 (sensory rhodopsin), or K04642 (halorhodopsin) models at or below an e-value of 1E-5 were retained for downstream analysis. Triplet motifs were extracted by alignment with characterized rhodopsin reference sequences (including BR).

A group of rhodopsin sequences with a novel DSE triplet motif were selected and further examined. First, scaffolds encoding DSE sequences were taxonomically profiled using annotations for all genes encoded on the scaffold. Phylum and order level affiliations were determined by the majority rule. The accuracy of predicted protein sequences was then verified by re-mapping of the original metagenomic reads to assembled scaffolds followed by manual curation to identify assembly errors. Finally, the genomic context for novel DSE rhodopsins was examined by secondary annotation of neighboring genes with kofamscan at a more stringent threshold (e≤1E-20) and visualized using gggenes.

Construction of DNA Plasmids for DSE Expression

The genes encoding DSE rhodopsins (DSE428 (from Micrococcales), DSE009 (from Actinobacteria), DSE307 (Unknown)), with codons optimized for *Escherichia coli* expression, were synthesized using GenScript (Nanjing, China) (Supplementary Table S1) and cloned into NdeI–XhoI site of the pET21a (+) vector (Novagen, Merck KGaA, Germany). The plasmids were transformed into *E. coli* C43 (DE3) strain (Lucigen, WI). For mutagenesis, the QuikChange site-directed mutagenesis method (Agilent Technologies, CA) was employed according to a standard protocol. The primer sequences used for mutagenesis are listed in Supplementary Table S2.

Protein Expression and Purification

E. coli cells harboring the DSE-cloned plasmids were cultured in 2×YT medium containing 50 μg/mL ampicillin. The expression of C-terminal 6× His-tagged proteins was induced by 0.1 mM IPTG in the presence of 10 μM all-*trans*-retinal (Toronto Research Chemicals, Canada) at 37 °C for 4 h.

Proton Transport Activity Assay

Rhodopsin-expressing *E. coli* cells were collected through centrifugation at 4,800 ×*g* at 20 °C for 2 min (CF15RF; Eppendorf Himac Technologies, Japan) and washed with 100 mM NaCl. The cells were equilibrated three times with rotational mixing in 100 mM NaCl at room temperature for 10 min. Finally, the cells were suspended in 7.5 mL of unbuffered 100 mM NaCl and the optical density (OD) at 600 nm was adjusted to 2. The cell suspension was placed in the dark in a glass cell at 20 °C and illuminated at $\lambda = 520 \pm 10$ nm from the output of a 300 W xenon light source (MAX-303; Asahi Spectra, Japan) through band-pass (F10-520.0-4-1.00, CVI Melles Griot) and heat-absorbing (HAF-50S-50H; SIGMAKOKI, Japan) filters. Light-induced pH changes were measured using a pH electrode (9618S-10D; HORIBA, Japan). The measurements were repeated under the same conditions after the addition of carbonyl cyanide *m*-chlorophenylhydrazone (CCCP, final concentration = 10 μM).

Hydroxylamine Bleaching

To quantitatively compare ion transport activity, the amount of protein was determined by measuring the near-UV absorption of retinal oxime generated by the hydrolysis reaction between the retinal Schiff base (RSB) in the proteins and hydroxylamine (HA). Briefly, rhodopsin-expressing *E. coli* cells were washed with a buffer containing 133 mM NaCl and 66.5 mM Na_2HPO_4 (pH 8.0). The washed cells were treated with 1 mM lysozyme and a small amount of DNaseI for 1 h and disrupted through sonication. To solubilize rhodopsins, 3% n-dodecyl-β-D-maltopyranoside (DDM) was added, and the samples were stirred overnight at 4 °C. The rhodopsins were bleached with 50 mM HA and illuminated with visible light ($\lambda > 500$ nm) from the output of a 300 W xenon lamp (MAX-303, Asahi Spectra, Japan) through long-pass (Y-52; AGC Techno Glass, Japan) and heat-absorbing (HAF-50S-50H, SIGMAKOKI, Japan) filters. The absorption changes due to the bleaching of rhodopsin by the hydrolysis reaction between retinal and HA and the formation of retinal oxime were measured using a UV–visible spectrometer (V-750; JASCO, Japan). The molecular extinction coefficient (ε) of rhodopsin was calculated as the ratio between the absorbance of rhodopsin and retinal oxime ($\varepsilon = 33{,}900\ M^{-1}\ cm^{-1}$) [27], and the amount of rhodopsin expressed in *E. coli* cells was determined by the absorbance of bleached rhodopsin and its ε. Relative ion transport activities were normalized to the relative amounts of expressed proteins.

Protein Purification

To investigate the photoreaction of DSE rhodopsins, DSE009 was chosen as a representative sample of DSE rhodopsin protein set, and it was purified. The harvested cells were sonicated (Ultrasonic Homogenizer VP-300N; TAITEC, Japan) for disruption in a buffer with 50 mM Tris–HCl (pH 8.0) and 5 mM $MgCl_2$. The membrane fraction was collected through ultracentrifugation (CP80NX; Eppendorf Himac Technologies, Japan) at 142,000 ×*g* for 1 h. The protein was solubilized in a buffer containing 50 mM MES–NaOH (pH 6.5), 300 mM NaCl, 5 mM imidazole, and 5 mM $MgCl_2$. After that, a second membrane fraction collection by ultracentrifugation at 142,000 ×*g* for 1 h was performed. Then, the protein was solubilized in a buffer containing 50 mM MES–NaOH (pH 6.5), 300 mM NaCl, 5 mM imidazole, 5 mM $MgCl_2$, and 3% DDM (ULTROL Grade; Calbiochem, Sigma-Aldrich, MO). Solubilized proteins were separated from the insoluble fractions through ultracentrifugation at 142,000 ×g for 1 h. Proteins were purified using a Ni-NTA affinity column (HisTrap HP His tag protein purification column with Ni Sepharose™ High Performance (HP) affinity resin; Cytiva, MA). The resin was washed with a buffer containing 50 mM MES–NaOH (pH 6.5), 300 mM NaCl, 50 mM imidazole, 5 mM $MgCl_2$, and 0.1% DDM. Proteins were eluted in a buffer containing 50 mM Tris–HCl (pH 7.0), 500 mM NaCl, 500 mM imidazole, 5 mM $MgCl_2$, and 0.1% DDM. The eluted protein was dialyzed in a buffer containing 50 mM Tris–HCl (pH 8.0), 100 mM NaCl, and 0.05% DDM to remove imidazole.

pH Titration

To investigate the pH dependence of the absorption spectra of DSE009, the concentration of protein was adjusted to OD = ~0.5 at λ^a_{max} and solubilized in a 6-mix buffer (trisodium citrate, MES, HEPES, MOPS, CHES, CAPS (10 mM each, pH 7.0), 100 mM NaCl, and 0.05% DDM). The pH was adjusted to the desired value by the addition of small aliquots of HCl and NaOH. Absorption spectra were recorded using a UV–vis spectrometer (V-750, JASCO, Japan). The measurements were performed at every 0.3–0.6 pH values.

Laser Flash Photolysis

The details of the laser flash photolysis system have been reported [5,24]. DSE009 was purified and sample solution was exchanged with a buffer containing 20 mM HEPES−NaOH (pH 7.0), 100 mM NaCl, and 0.05% DDM. The absorption

of the protein solution was adjusted to ~0.5 (total protein concentration of ~0.25 mg mL^{-1}) at an excitation wavelength of 532 nm. The sample was illuminated with a beam of second harmonics of a nanosecond-pulsed Nd:YAG laser (λ = 532 nm, 5.7 mJ cm^{-2}, 0.025–1 Hz) (INDI40; Spectra-Physics, CA, USA). The time evolution of the transient absorption change was obtained by observing the intensity change of the output of a xenon arc lamp (L9289-01; Hamamatsu Photonics, Japan) monochromated by a monochromator (S-10; SOMA OPTICS, Japan) and passed through the sample after photoexcitation using a photomultiplier tube (R10699; Hamamatsu Photonics, Japan) equipped with a notch filter (532 nm, bandwidth = 17 nm) (Semrock, NY) to remove the scattered pump pulse. To increase the signal-to-noise ratio (SNR), 10–20 signals were averaged. The signals were globally fitted with a multi-exponential function to determine the lifetimes and absorption spectra of each photointermediate.

Results

Light-Driven H^+ Transport Activity Assay by DSE Rhodopsins

To investigate the ion transport function of three DSE rhodopsins (DSE428, 009, and 307), all proteins were expressed in *E. coli* cells. All cells showed orangish colors, indicating the formation of functional rhodopsins with the retinal chromophore. The H^+ transport activity of *E. coli* cells was assayed by observing light-induced pH changes of the external solvent, as it was employed previously [24,28] and the results are summarized in Figure 2A. A cell suspension of *E. coli* expressing H^+ pump shows acidification (pH decrease) or alkalinization (pH increase) of the external medium upon illumination by outward or inward H^+ transport, respectively, and the signals are eliminated in the presence of a protonophore, CCCP. Although the expressed proteins exhibited orangish colors indicating blue–green light absorbing property, DSE428 and DSE307 did not show any ion transport activity. Only an extremely small outward H^+ pump activity, *i.e.*, acidification or pH decrease, of the external solvent upon illumination was observed in the case of DSE009 (Figure 2A). The signal was eliminated in the presence of CCCP indicating it derived from the outward H^+ transport by DSE009.

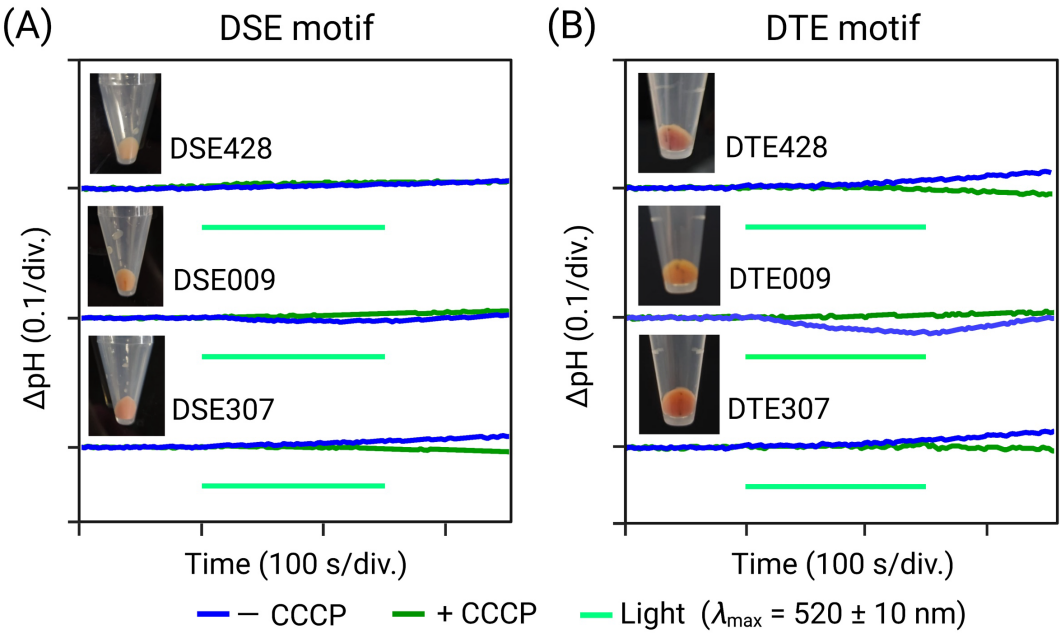

Figure 2 Light-driven active H^+ transport by DSE rhodopsins and their DTE-motif mutants. (A, B) H^+ transport activity assay of DSE rhodopsins (A) and their DTE-motif mutants (B) in *E. coli* cells without (blue) and with (green) 10 μM CCCP. The cells were illuminated with light (λ = 520 ± 10 nm) for 150 s (light green). The pictures of the pellets of *E. coli* cells expressing DSE rhodopsins and DTE-motif mutants were shown next to the corresponding results.

Although the DSE motif is different from the DTD or DTE motifs, which are the most common among the outward H^+ pumping rhodopsins, serine and threonine have similar chemical character. The weak outward H^+ pumping function of DSE009 is consistent with this chemical similarity, and the DTE motif is more effective to achieve higher transport activity. With this motivation, we constructed the DTE motif by site-directed mutagenesis for these three DSE rhodopsins (DTE428, 009, and 307) and evaluated their H^+ transport activity (Figure 2B). The signal was slightly enhanced for DTE009, whereas DTE428 and DTE307 still did not display any ion transport activity.

Absorption Spectra of DSE Rhodopsins

To quantify the absorption properties of DSE rhodopsins, the samples were illuminated in the presence of HA. This photoreaction process converts the protein-bound retinal chromophore into retinal oxime which will be released, so that one can easily obtain the absorption maximum wavelength (λ^{a}_{max}) of each protein without purification by calculating the difference absorption spectra between after and before the reaction with HA. Figure 3A shows the result representing the photobleaching of DSE428, 009, and 307 in the presence of 50 mM HA (see "Material and Methods" section). Two positive peaks at around 545 nm (except for DSE307, which this same positive peak appears around 514 nm) and 420 nm corresponding to the unphotolyzed protein and one negative peak at 350–360 nm corresponding to retinal oxime were observed. The positive peak at > 500 nm and ~420 nm represents the unphotolyzed protein with protonated RSB and deprotonated RSB, respectively. Whereas the former is considered to represent functional state as many other rhodopsins, the latter would represent unfunctional state or be originated from denatured protein. Although protein pellets showed orangish colors (Figure 2A), what can make us hypothesize blue–green light absorbing property, DSE428 and DSE009 rhodopsins displayed λ^{a}_{max} above 540 nm, while DSE307 presented the most blueshifted λ^{a}_{max} value compared with the other two DSE rhodopsins. This spectral blueshift observed in DSE307 with respect the other studied DSE rhodopsins could be motivated by the different amino acid residues present close to the Schiff base (SB) (Supplementary Figure S1). Next to the lysine residue, which is linked to the retinal chromophore (Supplementary Figure S1, purple diamond), DSE428 and DSE009 conserve the same alanine residue as in BR and GR. However, in the case of DSE307, this alanine is substituted by a serine residue. Consistent with the color tuning theory described in the literature [29,30], such polar amino acid residue, placed near the RSB, would cause a spectral blueshift. The similar spectral blueshift was observed for DTE307 compared with the other two DTE mutants (Figure 3B). In addition, we observed a systematic blueshift in all the DTE mutants with respect to original DSE rhodopsins, especially the strongest blueshift was observed between DSE009 and DTE009 (14-nm shift), suggesting slight structural difference between serine and threonine with an additional methyl group in the latter can change the electronic state of the retinal substantially.

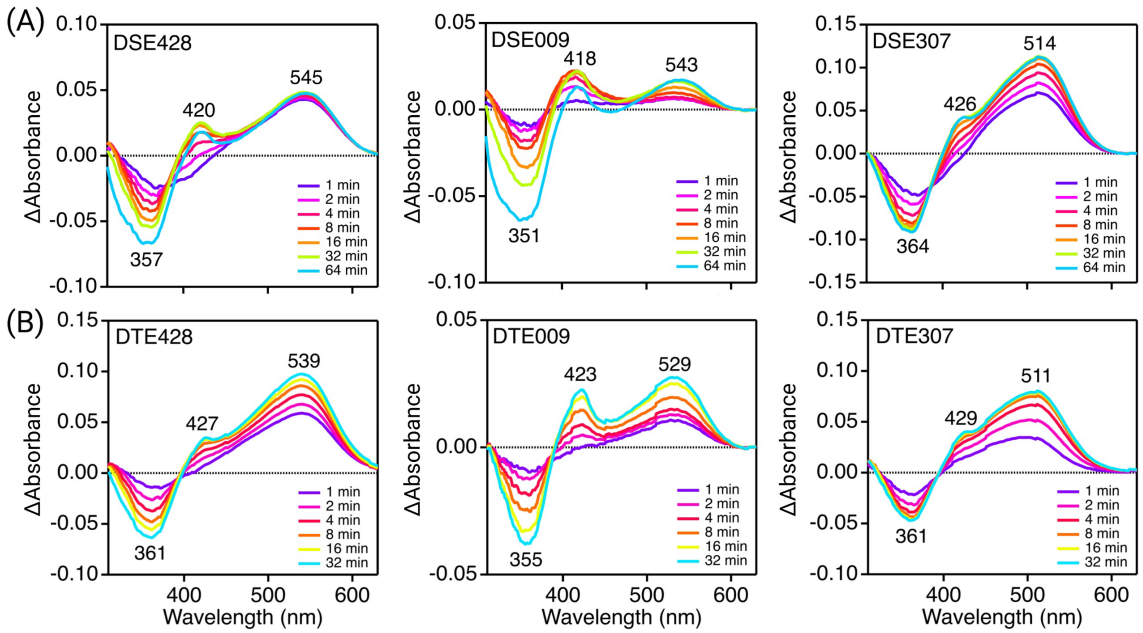

Figure 3 (A, B)Light-induced difference absorption spectra of DSE rhodopsins (A) and their DTE mutants (B) in the presence of 50 mM HA. The difference in absorption spectra before and after HA bleaching reactions of DSE rhodopsins and DTE mutants in solubilized *E. coli* membranes. The λ^{a}_{max} of each DSE rhodopsin and DTE mutant was determined by the positions of the absorption indicated in each panel, and the absorption of retinal oxime produced by the hydrolysis reaction of RSB, and HA was observed as negative peaks in the proximity of 360–370 nm. The reaction proceeded with light (λ > 500 nm) illumination for up to 64 min for DSE motif rhodopsins and 32 min for DTE motif rhodopsins.

Absorption Spectra and Photocycle of DSE009

To further study the molecular properties of DSE rhodopsins, we purified and spectroscopically investigated DSE009 which exhibited substantial H^+ pump activity. The absorption spectrum of purified DSE009 exhibited λ^{a}_{max} of 536 nm in detergent (DDM) (Figure 4A). The absorption peak was highly redshifted at acidic pH (from 536 to 562 nm)

(Supplementary Figure S2A). This redshift in the λ^{a}_{max} value was caused by the protonation of the primary counterion (*i.e.,* the aspartic acid in the DSE motif) (Figure 4B). On the other hand, at alkaline pH (Supplementary Figure S2B), this peak moved to the near-UV region, indicating the deprotonation of the RSB. By fitting the absorption change with the Henderson–Hasselbalch equation [31], the pK_a values of the counterion and RSB were estimated. While the former was 1.28 ± 0.01, the RSB exhibited two-step deprotonation with pK_{a1} = 9.1 ± 0.7 and pK_{a2} = 11.988 ± 0.008, respectively (Figure 4B and C).

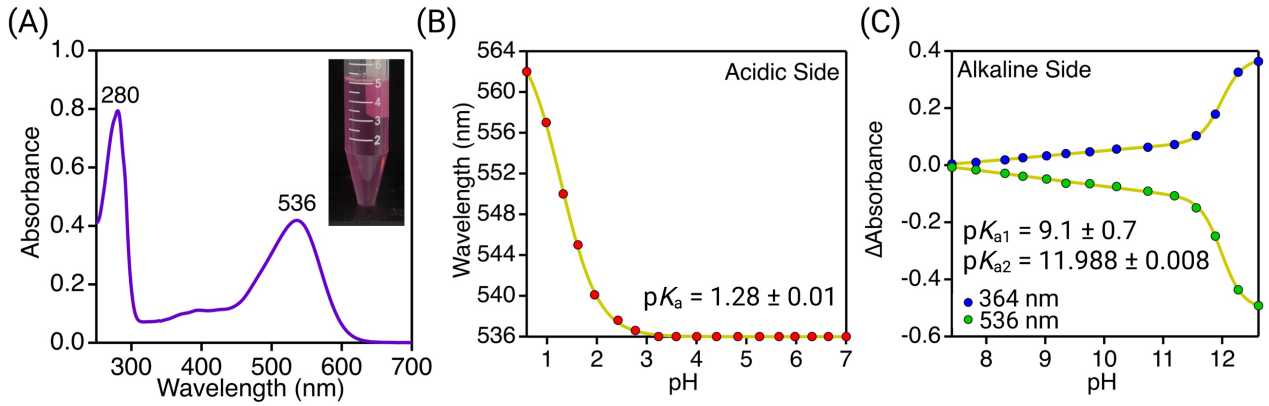

Figure 4 Absorption spectrum of purified DSE009 and pH dependence of the absorption. (A) UV-vis absorption spectrum in 20 mM HEPES−NaOH (pH 7.0), 100 mM NaCl, and 0.05% DDM. The picture of the purified protein is shown next to the corresponding result. The purified DSE009 showed λ^{a}_{max} of 536 nm in DDM. (B) and (C) Absorption change representing protonated (B) and deprotonated (C) RSB at different pH. pK_a values were estimated by fitting the absorption change with the Henderson–Hasselbalch equation [31]. Especially, the global fitting was performed against the absorption changes at two different wavelengths in (C). The protein was solubilized in 100 mM NaCl, 6-mix buffer (trisodium citrate, MES, HEPES, MOPS, CHES, and CAPS (10 mM each)), and 0.05% DDM.

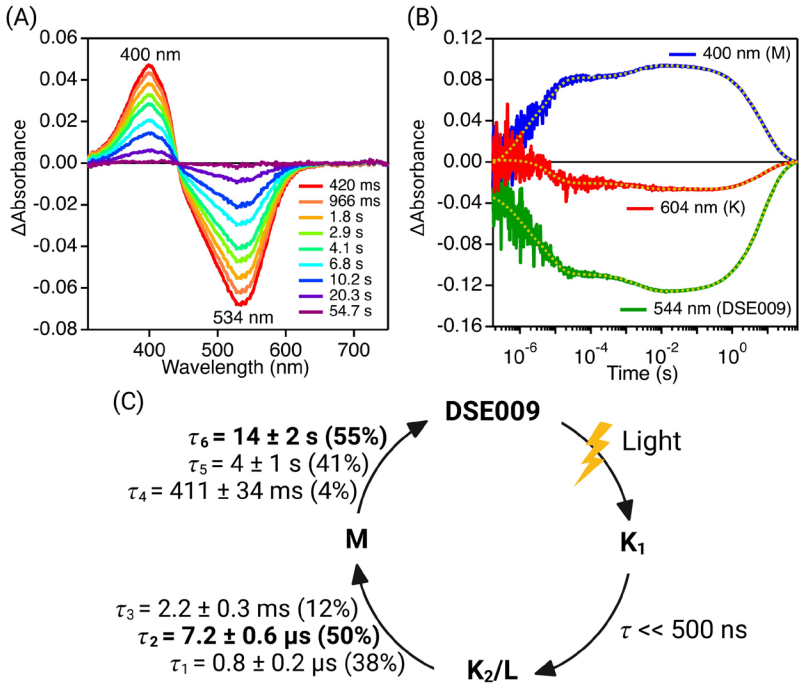

Figure 5 Transient absorption changes and the photocycles of DSE009. (A) Transient absorption spectra, (B) time evolution of transient absorption changes at specific probe wavelengths, and (C) photocycle model determined by analyzing the time evolution with multiexponential functions (dashed yellow lines in figure B, Supplementary Table S3) in a buffer containing 20 mM HEPES−NaOH (pH 7.0), 100 mM NaCl, and 0.05% DDM. The most dominant components in multi-exponential process were highlighted in bold.

We next studied the photocycle reaction of DSE009 by the laser flash photolysis, in which the DSE009 protein was solubilized in DDM (Figure 5). Figure 5A shows the transient change in absorption of DSE009 upon excitation at λ = 532 nm, representing the accumulation of photointermediates at 400 nm similar to BR's M intermediates [32]. Simultaneously, the full bleaching signal at λ = 534 nm was observed indicating only the M intermediate accumulated at $t \geq 420$ ms. To monitor the transient absorption change representing short-lived intermediates prior to the M, we conducted measurement at specific probe wavelengths with a photomultiplier tube at higher time resolution (Figure 5B). The decays of K and L intermediates are represented by the decrease in absorption at 544 and 604 nm, respectively (Figure 5B). The triple exponential decay in the K/L had lifetimes of τ = 0.8 µs, 7.2 µs, and 2.2 ms, and the accumulation of the blueshifted M intermediate was observed simultaneously at 400 nm (Figure 5B–C, Supplementary Table S3). The decay of M was also well reproduced with a triple exponential function with the lifetimes of τ = 411 ms, 4 s, and 14 s (Figure 5C, Supplementary Table S3). As in other sensory rhodopsins [33,34], the last long-lived M photointermediate in DSE009 could correspond to the signaling state as photosensor. The turnover rate of the photocycle reaction of the purified protein was extremely slow compared to canonical H^+ pumping rhodopsins typically in several tens to hundreds milliseconds [35] (Figure 5C), suggesting these new rhodopsins could function as photosensors, such as sensory rhodopsins [36,37] (Supplementary Figure S1), or H^+ pumps whose activities are enhanced by currently unknown regulatory systems in the genome [38].

Genomic Context of DSE Rhodopsins

Annotation of neighboring genes revealed that DSE rhodopsins in Actinobacteria are frequently surrounded by putative serine/threonine protein kinases (K08884), putative agmatine deiminases (K10536), and putative para-nitrobenzyl esterases (K03929) (Figure 6). In some cases, multiple genes likely encoding serine/threonine protein kinases were found in the immediate vicinity, although not always in the same strand as that encoding the rhodopsin (Figure 6). Notably, no incidences of brp/blh, the gene required for the synthesis of the retinal cofactor essential to functioning rhodopsin, were found within 5 kbp of the rhodopsin.

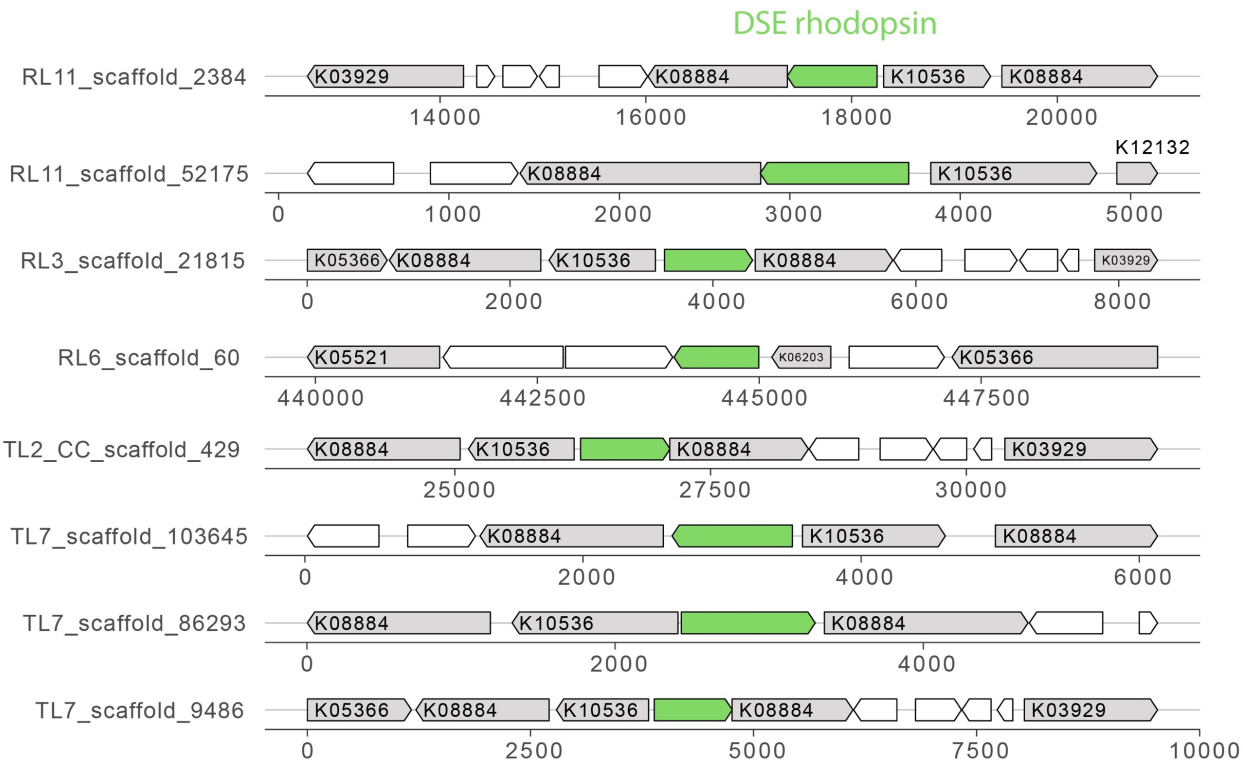

Figure 6 Genomic context for a subset of DSE rhodopsins (indicated in green). Neighboring genes that could be confidently annotated by KEGG are indicated in gray along with the highest scoring hidden Markov model (HMM) model. Genes that could not be confidently annotated are indicated in white. Numbers below gene diagrams indicate the genomic coordinates along the encoding scaffold.

Discussion

DSE motif rhodopsins were first identified in the members of Actinobacteria, primarily of the order Micrococcales and are in phylogenetically positions distinct from typical microbial rhodopsins groups (Figure 1). The novel DSE motif is unique among microbial rhodopsins. For this reason, it is difficult to figure out the function of DSE rhodopsins. The well-studied outward H^+ pumping rhodopsins, BR and proteorhodopsin (PR) [39], possess the characteristic DTD and DTE motifs, respectively, in which the first D is a counterion of the protonated RSB and also works as the proton acceptor from it (Asp85 for BR, see Supplementary Figure S1). The third D and E in BR and PR, respectively, are the proton donor for the Schiff base reprotonation (Asp96 for BR, see Supplementary Figure S1). This amino acid-residue configuration is also observed in DSE rhodopsins. Based on this reasoning, DSE rhodopsins could be also candidates to exhibit a light-driven H^+ pump function as BR and PR. The present light-driven H^+ transport assay experiments demonstrated that only DSE009 rhodopsin showed an extremely small outward H^+ pump activity (Figure 2A). Since DSE rhodopsins possess a serine residue instead a threonine, which is the most popular one among the outward H^+ pumping rhodopsins and it is a critical element in the H^+ transfer between the RSB and the proton acceptor [15], the light-driven H^+ transport assay experiments were conducted again with the construction of the DTE motif in DSE rhodopsins by site-directed mutagenesis (Figure 2B). However, again, only DTE009 presented an enhancement for the signal with respect to the other two DSE rhodopsins. Although this short experiment revalidated the importance of the presence of threonine in the outward H^+-pumping rhodopsin motifs, it is not enough to achieve higher H^+ pumping activity as canonical H^+ pumps.

Based on the orangish color of the expressed proteins (Figure 2), which is an indicative of the blue–green absorbing property, one can hypothesize an optimal outward H^+ pump activity. Hoverer, this did not happen like that and no or extremely small outward H^+ pump activity was observed (Figure 2A). To find a reason, HA bleach method was employed to quantify the absorption properties of DSE rhodopsins (Figure 3). DSE428 and DSE009 rhodopsins displayed λ^{a}_{max} values above 540 nm, while DSE307 presented the most blueshifted λ^{a}_{max} value at 514 nm compared with the other two DSE rhodopsins. The color tuning mechanism has been extensively studied in microbial rhodopsins, and several mutation studies have experimentally revealed key residues [40,41]. One of the color determinant residues is Ala215 in BR (Supplemenatry Figure S1), and the introduction of a polar amino acid residue such a serine or threonine causes a spectral blueshift about 20 nm. Unlike the other two DSE rhodopsins which possess alanine, DSE307 possesses a serine at this position nearby the lysine linked to the all-*trans*-retinal chromophore (Supplementary Figure S1). Therefore, threonine at this position must contribute to the blueshifted absorption of DSE307 (Figure 3A). The same behavior was also observed in the mutated DTE rhodopsins (Figure 3B). This is fully consistent with the idea that the polarity at the position is the color determinant even in DSE rhodopsins and it is diversified according to each environment.

DSE009 was chosen as the representative protein of DSE rhodopsins to study the molecular properties of DSE rhodopsins because it was the only one which displayed a considerable H^+ pump activity. Purified DSE009 rhodopsin absorbs maximally at 536 nm (Figure 4A). In a flash photolysis study of DSE009, the formation of the K, L and M intermediates was observed (Figure 5), which is also common among microbial rhodopsins. The turnover rate of the photocycle reaction of the purified proteins was extremely slow compared to typical H^+ pumping rhodopsins, suggesting these new rhodopsins would work as photosensors or H^+ pumps whose activities are enhanced by an unknown regulatory system in the hosts.

Our results suggest that diverse terrestrial lichens harbor microbiomes that include Actinobacteria encoding light-sensitive proteins (Figure 6). This finding is potentially consistent with the placement of lichen aggregates on the exterior of rocks and trees, where they experience transient or sustained sunlight during the day.

Conclusion

A new microbial rhodopsin group with a novel DSE motif was found in the members of the Actinobacteria. While a series of H^+ transfer similar to that of outward H^+ pumping rhodopsins, its turnover rate is very long resulting in either the no or small outward H^+ pump function. The genomic analyses found a common genomic clusters around DSE rhodopsin genes with putative serine/threonine protein kinases, putative agmatine deiminases, and putative para-nitrobenzyl esterases. DSE rhodopsins could either be involved in the cellular events related to signaling and/or metabolic reactions by these enzymes in a light dependent manner or function as an outward H^+ pump whose activity is regulated by an unknown system in the genome.

Conflict of Interest

The authors declare no competing financial interest.

Author Contributions

M.d.C.M. constructed DTE mutants, performed the expression of DSE and DTE proteins with *E. coli*, performed measurement of λ^{a}_{max} of the DSE and DTE rhodopsins, protein purification, pH-titration measurement, laser flash photolysis, experimental data analysis. M.K. advised the designing of experimental methods. A.L.J., P.T.W. and J.F.B. conducted sampling lichens and bioinformatic analyses of rhodopsins. M.d.C.M., A.L.J., J.F.B., and K.I. wrote the manuscript. All authors contributed to discussions and editing of the manuscript.

Data Availability

The evidence data generated and/or analyzed during the current study are available from the corresponding author on reasonable request.

Acknowledgements

We thank Prof. Oded Béjà at Technion – Israel Institute of Technology for the fruitful discussion about the microbiological significance of DSE rhodopsins. This work was supported by MEXT KAKENHI, Grant-in-Aid for Transformative Research Areas (B) "Low-energy manipulation" (Grant Number: JP20H05758 to K.I), JSPS KAKENHI, Grants-in-Aid (Grant Numbers: JP20F20081 to M.d.C.M., and JP21H01875, JP20K21383 to K.I.), and International Research Fellow of JSPS (Postdoctoral Fellowships for Research in Japan) to M.d.C.M. Sampling was performed at the Eel River Critical Zone Observatory, made possible by the National Science Foundation EAR 1331940.

References

[1] Ernst, O. P., Lodowski, D. T., Elstner, M., Hegemann, P., Brown, L. S., Kandori, H. Microbial and animal rhodopsins: Structures, functions, and molecular mechanisms. Chem. Rev. 114, 126–163 (2014). https://doi.org/10.1021/cr4003769

[2] Nagata, T., Inoue, K. Rhodopsins at a glance. J. Cell Sci. 134, jcs258989 (2021). https://doi.org/10.1242/jcs.258989

[3] Rozenberg, A., Inoue, K., Kandori, H., Béjà, O. Microbial rhodopsins: The last two decades. Annu. Rev. Microbiol. 75, 427–447 (2021). https://doi.org/10.1146/annurev-micro-031721-020452

[4] De Grip, W. J., Ganapathy, S. Rhodopsins: An excitingly versatile protein species for research, development and creative engineering. Front. Chem. 10, 1–48 (2022). https://doi.org/10.3389/fchem.2022.879609

[5] Inoue, K., Ono, H., Abe-Yoshizumi, R., Yoshizawa, S., Ito, H., Kogure, K., et al. A light-driven sodium ion pump in marine bacteria. Nat. Commun. 4, 1678 (2013). https://doi.org/10.1038/ncomms2689

[6] Govorunova, E. G., Sineshchekov, O. A., Li, H., Spudich, J. L. Microbial rhodopsins: Diversity, mechanisms, and optogenetic applications. Annu. Rev. Biochem. 86, 845–872 (2017). https://doi.org/10.1146/annurev-biochem-101910-144233

[7] Mukherjee, S., Hegemann, P., Broser, M. Enzymerhodopsins: novel photoregulated catalysts for optogenetics. Curr. Opin. Struct. Biol. 57, 118–126 (2019). https://doi.org/10.1016/j.sbi.2019.02.003

[8] Rozenberg, A., Kaczmarczyk, I., Matzov, D., Vierock, J., Nagata, T., Sugiura, M., et al. Rhodopsin–bestrophin fusion proteins from unicellular algae form gigantic pentameric ion channels. Nat. Struct. Mol. Biol. 29, 592–603 (2022). https://doi.org/10.1038/s41594-022-00783-x

[9] Philosof, A., Béjà, O. Bacterial, archaeal and viral-like rhodopsins from the Red Sea. Environ. Microbiol. Rep. 5, 475–482 (2013). https://doi.org/10.1111/1758-2229.12037

[10] Beja, O., Aravind, L., Koonin, E. V., Suzuki, M. T., Hadd, A., Nguyen, L. P., et al. Bacterial rhodopsin: Evidence for a new type of phototrophy in the sea. Science 289, 1902–1906 (2000). https://doi.org/10.1126/science.289.5486.1902

[11] Venter, J. C., Remington, K., Heidelberg, J. F., Halpern, A. L., Rusch, D., Eisen, J. A., et al. Environmental genome shotgun sequencing of the Sargasso Sea. Science 304, 66–74 (2004). https://doi.org/10.1126/science.1093857

[12] Olson, D. K., Yoshizawa, S., Boeuf, D., Iwasaki, W., DeLong, E. F. Proteorhodopsin variability and distribution in the North Pacific Subtropical Gyre. ISME J. 12, 1047–1060 (2018). https://doi.org/10.1038/s41396-018-0074-4

[13] Oesterhelt, D., Stoeckenius, W. Rhodopsin-like protein from the purple membrane of *Halobacterium halobium*. Nature 233, 149–152 (1971). https://doi.org/10.1038/newbio233149a0

[14] Mogi, T., Stern, L. J., Marti, T., Chao, B. H., Khorana, H. G. Aspartic acid substitutions affect proton translocation by bacteriorhodopsin. Proc. Natl. Acad. Sci. U.S.A. 85, 4148–4152 (1988). https://doi.org/10.1073/pnas.85.12.4148

[15] Bondar, A.-N., Fischer, S., Smith, J. C., Elstner, M., Suhai, S. Key role of electrostatic interactions in bacteriorhodopsin proton transfer. J. Am. Chem. Soc. 126, 14668–14677 (2004). https://doi.org/10.1021/ja047982i
[16] Inoue, K., Kato, Y., Kandori, H. Light-driven ion-translocating rhodopsins in marine bacteria. Trends Microbiol. 23, 91–98 (2015). https://doi.org/10.1016/j.tim.2014.10.009
[17] Petrovskaya, L. E., Lukashev, E. P., Chupin, V. V., Sychev, S. V., Lyukmanova, E. N., Kryukova, E. A., et al. Predicted bacteriorhodopsin from Exiguobacterium sibiricum is a functional proton pump. FEBS Lett. 584, 4193–4196 (2010). https://doi.org/10.1016/j.febslet.2010.09.005
[18] Harris, A., Ljumovic, M., Bondar, A.-N., Shibata, Y., Ito, S., Inoue, K., et al. A new group of eubacterial light-driven retinal-binding proton pumps with an unusual cytoplasmic proton donor. Biochim. Biophys. Acta Bioenerg. 1847, 1518–1529 (2015). https://doi.org/10.1016/j.bbabio.2015.08.003
[19] Maliar, N., Okhrimenko, I. S., Petrovskaya, L. E., Alekseev, A. A., Kovalev, K. V, Soloviov, D. V, et al. Novel pH-sensitive microbial rhodopsin from *Sphingomonas paucimobilis*. Dokl. Biochem. Biophys. 495, 342–346 (2020). https://doi.org/10.1134/S1607672920060162
[20] Matsuno-Yagi, A., Mukohata, Y. Two possible roles of bacteriorhodopsin; a comparative study of strains of *Halobacterium halobium* differing in pigmentation. Biochem. Biophys. Res. Commun. 78, 237–243 (1977). https://doi.org/10.1016/0006-291X(77)91245-1
[21] Hasemi, T., Kikukawa, T., Kamo, N., Demura, M. Characterization of a cyanobacterial chloride-pumping rhodopsin and its conversion into a proton pump. J. Biol. Chem. 291, 355–362 (2016). https://doi.org/10.1074/jbc.M115.688614
[22] Nakajima, Y., Tsukamoto, T., Kumagai, Y., Ogura, Y., Hayashi, T., Song, J., et al. Presence of a haloarchaeal halorhodopsin-like Cl^- pump in marine bacteria. Microbes Environ. 33, 89–97 (2018). https://doi.org/10.1264/jsme2.ME17197
[23] Yoshizawa, S., Kumagai, Y., Kim, H., Ogura, Y., Hayashi, T., Iwasaki, W., et al. Functional characterization of flavobacteria rhodopsins reveals a unique class of light-driven chloride pump in bacteria. Proc. Natl. Acad. Sci. U.S.A. 111, 6732–6737 (2014). https://doi.org/10.1073/pnas.1403051111
[24] Inoue, K., Tsunoda, S. P., Singh, M., Tomida, S., Hososhima, S., Konno, M., et al. Schizorhodopsins: A family of rhodopsins from Asgard archaea that function as light-driven inward H^+ pumps. Sci. Adv. 6, aaz2441 (2020). https://doi.org/10.1126/sciadv.aaz2441
[25] Inoue, K., Ito, S., Kato, Y., Nomura, Y., Shibata, M., Uchihashi, T., et al. A natural light-driven inward proton pump. Nat. Commun. 7, 13415 (2016). https://doi.org/10.1038/ncomms13415
[26] Li, D., Liu, C.-M., Luo, R., Sadakane, K., Lam, T.-W. MEGAHIT: An ultra-fast single-node solution for large and complex metagenomics assembly via succinct *de Bruijn* graph. Bioinformatics 31, 1674–1676 (2015). https://doi.org/10.1093/bioinformatics/btv033
[27] Scharf, B., Hess, B., Engelhard, M. Chromophore of sensory rhodopsin II from *Halobacterium halobium*. Biochemistry 32, 3830 (1993). https://doi.org/10.1021/bi00065a045
[28] Inoue, K., Nomura, Y., Kandori, H. Asymmetric functional conversion of eubacterial light-driven ion pumps. J. Biol. Chem. 291, 9883–9893 (2016). https://doi.org/10.1074/jbc.M116.716498
[29] Oded, B., Spudich, E. N., Spudich, J. L., Leclerc, M., DeLong, E. F. Proteorhodopsin phototrophy in the ocean. Nature 411, 786–789 (2001). https://doi.org/10.1074/jbc.M116.716498
[30] Inoue, K., Tsukamoto, T., Sudo, Y. Molecular and evolutionary aspects of microbial sensory rhodopsins. Biochim. Biophys. Acta Bioenerg. 1837, 562–577 (2014). https://doi.org/10.1016/j.bbabio.2013.05.005
[31] Po, H. N., Senozan, N. M. The Henderson-Hasselbalch equation: Its history and limitations. J. Chem. Educ. 78, 1499–1503 (2001). https://doi.org/10.1021/ed078p1499
[32] Chizhov, I., Chernavskii, D. S., Engelhard, M., Mueller, K. H., Zubov, B. V., Hess, B. Spectrally silent transitions in the bacteriorhodopsin photocycle. Biophys. J. 71, 2329–2345 (1996). https://doi.org/10.1016/S0006-3495(96)79475-4
[33] Yan, B., Takahashi, T., Johnson, R., Spudich, J. L. Identification of signaling states of a sensory receptor by modulation of lifetimes of stimulus-induced conformations: The case of sensory rhodopsin II. Biochemistry 30, 10686–10692 (1991). https://doi.org/10.1021/bi00108a012
[34] Kondoh, M., Inoue, K., Sasaki, J., Spudich, J. L., Terazima, M. Transient dissociation of the transducer protein from *Anabaena* sensory rhodopsin concomitant with formation of the M state produced upon photoactivation. J. Am. Chem. Soc. 133, 13406–13412 (2011). https://doi.org/10.1021/ja202329u
[35] Inoue, K. Diversity, mechanism, and optogenetic application of light-driven ion pump rhodopsins in Optogenetics. Advances in Experimental Medicine and Biology (Yawo, H., Kandori, H., Koizumi, A., Kageyama, R. eds.) vol. 1293, pp. 89–126 (Springer, Singapore, 2021). https://doi.org/10.1007/978-981-15-8763-4_6
[36] Royant, A., Nollert, P., Edman, K., Neutze, R., Landau, E. M., Pebay-Peyroula, E., et al. X-ray structure of sensory

rhodopsin II at 2.1-Å resolution. Proc. Natl. Acad. Sci. U.S.A. 98, 10131–10136 (2001). https://doi.org/10.1073/pnas.181203898

[37] Kawanabe, A., Kandori, H. Photoreactions and structural changes of *Anabaena* sensory rhodopsin. Sensors 9, 9741–9804 (2009). https://doi.org/10.3390/s91209741

[38] Adam, A., Deimel, S., Pardo-Medina, J., García-Martínez, J., Konte, T., Limón, M. C., et al. Protein activity of the *Fusarium fujikuroi* rhodopsins CarO and OpsA and their relation to fungus-plant interaction. Int. J. Mol. Sci. 19, 215 (2018). https://doi.org/10.3390/ijms19010215

[39] Béjà, O., Aravind, L., Koonin, E. V, Suzuki, M. T., Hadd, A., Nguyen, L. P., et al. Bacterial rhodopsin: Evidence for a new type of phototrophy in the sea. Science 289, 1902–1906 (2000). https://doi.org/10.1126/science.289.5486.1902

[40] Shimono, K., Ikeura, Y., Sudo, Y., Iwamoto, M., Kamo, N. Environment around the chromophore in pharaonis phoborhodopsin: Mutation analysis of the retinal binding site. Biochim. Biophys. Acta Biomembr. 1515, 92–100 (2001). https://doi.org/10.1016/S0005-2736(01)00394-7

[41] Sudo, Y., Okazaki, A., Ono, H., Yagasaki, J., Sugo, S., Kamiya, M., et al. A blue-shifted light-driven proton pump for neural silencing. J. Biol. Chem. 288, 20624–20632 (2013). https://doi.org/10.1074/jbc.M113.475533